Appendix B

Additional Measurements

B.1 Comparison with the BCD technology

In this section, I present the measurements I have performed to compare the performances of the SPAD array detector used throughout all the experiments in this thesis, with a new SPAD array version, based on the Bipolar-CMOS-DMOS (BCD) technology (Table B.1). The switch from the CMOS to the BCD technology mainly leads to an increase in both the dark count rate (DCR) and the photon detection efficiency (PDE). Remarkably, the higher DCR should not represent a significant drawback in the context of applications for which the photon flux is not a major concern, e.g., the imaging of bright samples. On the other hand, it may hinder the possibility of performing measurements in the condition of very low photon budget, e.g., in the context of single molecule regime.

	CMOS based SPAD array	BCD based SPAD array
fill factor	$\approx 55\%$	57,5%
PDE, λ =450 nm	45%	53%
PDE, λ =650 nm	15%	35%
PDE, λ =850 nm	5%	7,5%
dark count rate	100 cps	5000 cps
time resolution (FWHM)	$<$ 200 ps	$<$ 80 ps
afterpulsing probability	2,5%	0,5%

Table B.1 **Comparison between BCD and CMOS versions of the SPAD array detector**. The afterpulsing probability for CMOS and BCD technology is reported for hold off set to 100 ns and 20 ns respectively.

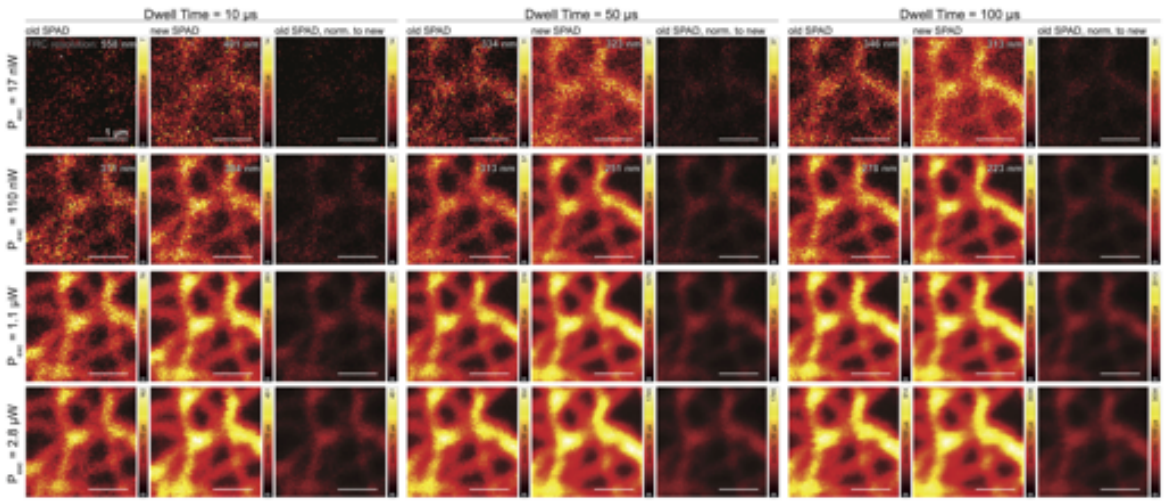

Figure B.1 **Comparison of the SPAD array detector based on the CMOS and BCD technology with tubulin imaging**. Details of a series of tubulin imaging experiments with increasing excitation powers and dwell times. For each dwell time, the last column represent the image obtained with the CMOS SPAD array detector, normalised to the BCD SPAD array image. The FRC resolution is also reported for the first two values of the excitation power. Pixel-dwell time: 10, 50, 100 μs. Pixel-size: 40 nm. Detail format: 70 $\times$ 70 pixels. Original image format: 250 $\times$ 250 pixels. Scale bars: 1 μm.

To validate the BCD SPAD array, I started imaging tubulin structures with increasing pixel dwell time, at increasing excitation powers P_{exc} (Fig. B.1). As expected, the increased PDE of the BCD SPAD array detector results in images with higher SNR, for every combination of dwell-time and excitation power, and the increased DCR does not represent a major concern. I then tested the performances of the novel BCD detector imaging a sample of nanorulers. Considering the few number of fluorophores linked to each DNA strand, this experiment resembles the condition of a single molecule measurement, such as single molecule tracking (see Chapter 7). Due to the severely reduced photon budget, the BCD SPAD array provided results with lower SNR with respect to the images obtained with the CMOS-based detector, in the condition of very low excitation power (P_{exc} =17 nW) and for each dwell-time tested. However, increasing the excitation power - and hence the photon flux - led to the BCD-based SPAD array detector providing higher SNR images with respect to the CMOS SPAD array (Fig. B.2).

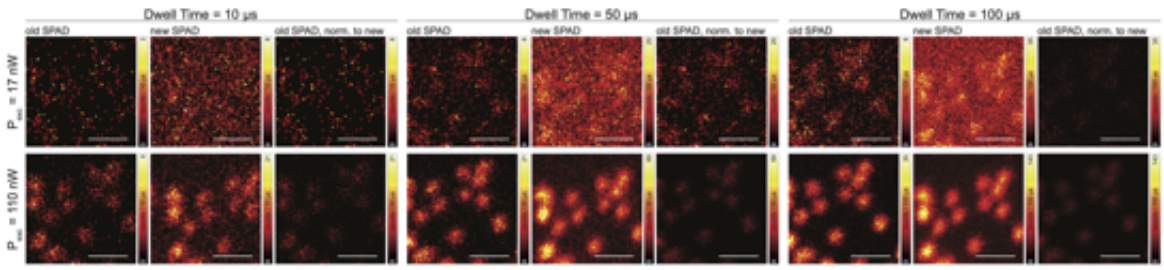

Figure B.2 **Comparison of the SPAD array detector based on the CMOS and BCD technology with nanoruler imaging**. Details of a series of nanoruler imaging experiments with increasing excitation powers and dwell times. For each dwell time, the last column represent the image obtained with the CMOS SPAD array detector, normalised to the BCD SPAD array image. Pixel-dwell time: 10, 50, 100 μs. Pixel-size: 40 nm. Detail format: 70 $\times$ 70 pixels. Original image format: 250 $\times$ 250 pixels. Scale bars: 1 μm.

B.2 Compatibility with fast resonant scanning

Fig. B.3 demonstrate the compatibility of the Image Scannning Microscopy setup based on the SPAD array with fast resonant scanning architectures. Notably, resonant scanning systems are normally combined with photomultiplier tubes, considering their higher dynamic range compared with that of SPADs. However, the effective dynamic range of the SPAD array is considerably higher than that of each single element, taking into account the spread of the photons across all the sensitive elements.

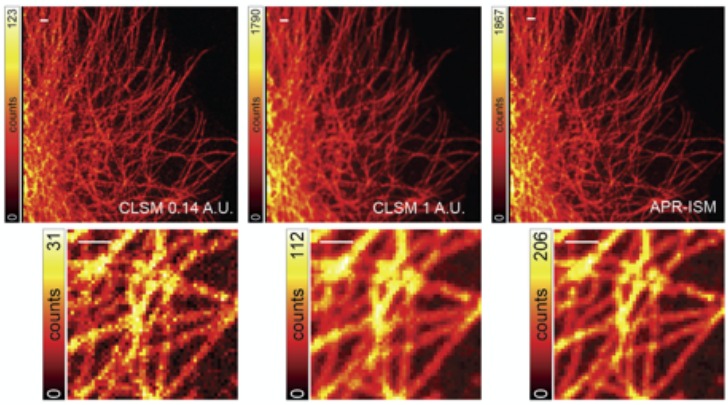

Figure B.3 **ISM combined with fast resonant scanning**. Side-by-side comparison between "ideal" confocal, "open" confocal and APR-ISM images of tubulin stained with Alexa Fluor 546. Image format: 256 $\times$ 256 pixels; resonant frequency, 7.9 kHz; zoom factor, 8, which results in a pixel size of 103 nm and a minimum pixel dwell time of about 70 ns; 64 line integrations. Insets show magnified views of the regions outlined by white boxes. Scale bars, 1 μm. Data are representative of $n = 10$ experiments.

Appendix C

List of Personal Publications

† Shared first author

C.1 Papers

- C. J. R. Sheppard, M. Castello, **G. Tortarolo**, T. Deguchi, S. V. Koho, G. Vicidomini, and A. Diaspro (2020). Pixel reassignment in image scanning microscopy: a re-evaluation, *Journal of the Optical Society of America A*, 37(1):154-162.
- M. Castello†, **G. Tortarolo**†, M. Buttafava, T. Deguchi, F. Villa, S. Koho, M. Oneto, S. Pelicci, L. Lanzanò, P. Bianchini, C. J. R. Sheppard, A. Diaspro, A. Tosi, and G. Vicidomini (2019). A robust and versatile platform for image scanning microscopy enabling super-resolution FLIM, *Nature Methods*, 16(2):175–178.
- **G. Tortarolo**, Y. Sun, K. Teng, Y. Ishitsuka, L. Lanzanó, P. R. Selvin, B. Barbieri, A. Diaspro and G. Vicidomini (2019). Photon-separation to enhance the spatial resolution in pulsed STED microscopy, *Nanoscale*, 11:1754-1761.
- S. Koho, **G. Tortarolo**, M. Castello, T. Deguchi, A. Diaspro, G. Vicidomini (2019). Fourier Ring/Shell Correlation measures dramatically simplify complex image restoration methods in fluorescence microscopy, *Nature Communications*, 10:3103.
- I. Coto, M. Castello, **G. Tortarolo**, N. Jowett, A. Diaspro, L. Lanzanò, G. Vicidomini (2019) Efficient two-photon excitation stimulated emission depletion nanoscope exploiting spatiotemporal information, *Neurophotonics*, 6(4):045004.
- **G. Tortarolo**†, M. Castello†, A. Diaspro, S. Koho and G. Vicidomini (2018). Evaluating image resolution in stimulated emission depletion microscopy, *Optica*, 5(1):32-35.
- C.J.R. Sheppard, M. Castello, **G. Tortarolo**, G. Vicidomini, A. Diaspro (2017). Image formation in image scanning microscopy, including the case of two-photon excitation, *Journal of the Optical Society of America A*, 34(8):1339-1350.
- M. Castello†, **G. Tortarolo**†, I. Coto Hernandez, T. Deguchi, A. Diaspro, and G. Vicidomini (2017). Removal of anti-Stokes emission background in STED microscopy by FPGA-based synchronous detection, *Review of Scientific Instruments*, 88:053701.

- S. Pelicci, **G. Tortarolo**, G. Vicidomini, A. Diaspro, L. Lanzanò (2020). Improving SPLIT-STED super-resolution imaging with tunable depletion and excitation power, *Journal of Physics D: Applied Physics*, under revision.

- **G. Tortarolo**, M. Castello, S. Koho, G. Vicidomini (2019). Synergic Combination of Stimulated Emission Depletion Microscopy with Image Scanning Microscopy to Reduce Light Dosage, *BioRxiv*, doi:https://doi.org/10.1101/741389.

- S.V. Koho†, E. Slenders†, **G. Tortarolo**, M. Castello, M. Buttafava, F. Villa, E. Tcarenkova, M. Ameloot, P. Bianchini, C.J.R. Sheppard, A. Diaspro, A. Tosi, G. Vicidomini (2019). Easy two-photon image-scanning microscopy with SPAD array and blind image reconstruction, *BioRxiv*, doi: https://doi.org/10.1101/563288.

C.2 Conference proceedings

- I. Coto, L. Lanzanó, M. Castello, N. Jowett, **G. Tortarolo**, A. Diaspro, G. Vicidomini (2018). Improving multiphoton STED nanoscopy with separation of photons by LIfetime Tuning (SPLIT), *Multiphoton Microscopy in the Biomedical Sciences XVIII, SPIE BIOS, vol. 10498.*

- Y. Sun†, **G. Tortarolo**†, K. W. Teng, Y. Ishitsuka, U. C. Coskun, S. J. Liao, A. Diaspro, G. Vicidomini, P. R. Selvin, B. Barbieri (2017). A novel pulsed STED microscopy method using FastFLIM and the phasor plots, *Multiphoton Microscopy in the Biomedical Sciences XVII, SPIE BIOS, vol. 10069.*

C.3 Oral contributions and posters

- **G. Tortarolo**, M. Castello, S. Koho, E. Slenders, A. Rossetta, M. Oneto, S. Pelicci, L. Lanzanò, A. Diaspro, and G. Vicidomini (2020). Time-resolved (STED) image scanning microscopy with a SPAD array, *talk, Focus on Microscopy 2020, Osaka.*

- **G. Tortarolo**, M. Castello, S. Koho, E. Slenders, A. Rossetta, A. Diaspro, and G. Vicidomini (2019). Fluorescence Laser Scanning Microscopy with SPAD Array: Exploiting the Extra Spatial And Temporal Information, *poster, Seeing is Believing 2019, EMBL Heidelberg.*

- **G. Tortarolo**, M. Castello, S. Koho, L. Pesce, M. Oneto, S. Pelicci, L. Lanzanó, A. Diaspro, and G. Vicidomini (2019). Stimulated Emission Depletion Image Scanning Microscopy with a SPAD Array, *talk, Focus on Microscopy 2019, London.*

- **G. Tortarolo**, M. Castello, M. Buttafava, T. Deguchi, F. Villa, S. Koho, P. Bianchini, C. J. R. Sheppard, A. Diaspro, A. Tosi, and G. Vicidomini (2018). Point-Scanning Microscopy with single-photon Detector Array, *talk, Workshop on Single Molecule Spectroscopy, Berlin.*

- **G. Tortarolo**, M. Castello, C. J. R. Sheppard, S. Koho, A. Diaspro, G. Vicidomini (2017). Fourier Ring Correlation as a tool to assess effective resolution in point scanning microscopy, *talk, Focus on Microscopy 2017, Bordeaux, France.*

C.4 Patent

- G. Vicidomini, M. Castello, **G. Tortarolo**, A. Tosi, M. Buttafava, F. Villa, P. Bianchini, A. Diaspro, C. J. R. Sheppard (2019). Time-resolved imaging method with high spatial resolution, *Patent pending, international pubblication number WO2019/145889 A1.*